

Jahn-Teller distortions and charge, orbital and magnetic orders in $\text{NaMn}_7\text{O}_{12}$

Sergey V. Streltsov^{1,2} and Daniel I. Khomskii³

¹*Institute of Metal Physics, S.Kovalevskoy St. 18, 620990 Ekaterinburg Russia*

²*Ural Federal University, Mira St. 19, 620002 Ekaterinburg, Russia**

³*II. Physikalisches Institut, Universität zu Köln, Zùlpicher Straße 77, D-50937 Köln, Germany*

With the use of the band structure calculations we demonstrate that previously reported [Nat. Materials **3**, 48 (2004)] experimental crystal and magnetic structures for $\text{NaMn}_7\text{O}_{12}$ are inconsistent with each other. The optimization of the crystal lattice allows us to predict a new crystal structure for the low temperature phase, which is qualitatively different from the one presented before. The AFM-CE type of the magnetic order stabilizes the structure with the elongated, not compressed $\text{Mn}_B^{3+}\text{O}_6$ octahedra, striking $\text{NaMn}_7\text{O}_{12}$ out of the list of the anomalous Jahn-Teller systems. The orbital correlations were shown to exist even in the cubic phase, while the charge order appears only in the low temperature distorted phase.

PACS numbers: 71.70.Ej, 61.50.Ah, 75.25.Dk

Introduction.— The quadruple perovskites based on transition metal (TM) ions with general formula $\text{A}'\text{A}''_3\text{B}_4\text{O}_{12}$ and mixed occupation of the A sites of initial ABO_3 perovskite structure by A' (cations with large ionic radii $\text{A}' = \text{La}, \text{Na}, \text{Ca}, \text{Bi}$ etc.), A'' (Jahn-Teller (JT) ions like Mn^{3+} , Cu^{2+}) ions are known for unusual physical properties. $\text{CaCu}_3\text{Ti}_4\text{O}_{12}$ shows a giant dielectric constant, [1] $\text{LaCu}_3\text{Fe}_4\text{O}_{12}$ demonstrates nontrivial charge ordering, [2] $\text{CaMn}_7\text{O}_{12}$ is multiferroic with the largest magnetically induced electric polarization measured to date, [3] associated with incommensurate structural modulations coupled with the rotation of the singly occupied e_g orbital of the Mn^{3+} ion. [4] The ferroelectric properties of another quadruple perovskite $\text{BiMn}_7\text{O}_{12}$ are also related to the orbital degrees of freedom, which is justified by the study of different doping regimes. [5]

The A site ordered quadruple perovskite $\text{NaMn}_3\text{Mn}_4\text{O}_{12}$ was shown to have intriguing properties. The authors of Ref. 6 argued that this system, which on octahedral B sites contains Mn ions with the average valence 3.5+, could be similar to half-doped manganites like $\text{La}_{0.5}\text{Ca}_{0.5}\text{MnO}_3$, and is better than the latter because it does not show disorder caused in the usual manganites by doping. Thus one could hope to get the “cleanest” signatures of charge and orbital order typical for half-doped manganites. And indeed, they discovered such ordering, occurring in $\text{NaMn}_7\text{O}_{12}$ at 180 K, but of completely different type. With further decrease of the temperature authors of Ref. 6 observed the same magnetic structure of the CE type (zigzag chains in the ac plane) as in the usual half-doped manganites.

The occupied orbitals of the JT Mn^{3+} ions in half-doped manganites are of $3x^2 - r^2$ and $3y^2 - r^2$ type, forming stripes in the basal plane, with locally elongated MnO_6 octahedra, long axes alternating in the x - and y -directions. In contrast, it was argued in Ref. 6 that in $\text{NaMn}_7\text{O}_{12}$ there exist local compression of these octahedra, with occupied orbitals being $x^2 - y^2$. This however is

very surprising. Local compression around JT ions with e_g degeneracy in insulators is extremely rare: among hundreds of known such systems there is practically none, or at best very few, examples with compressed octahedra. This is mostly due to the anharmonicity of the elastic interaction, and to higher-order Jahn-Teller coupling. [7–9]

Thus, the compounds with compressed Jahn-Teller octahedra for the case of e_g degeneracy is a very rare phenomenon, and there must be special reasons for such distortions - for example the layered structure, as in $\text{La}_{0.5}\text{Sr}_{1.5}\text{MnO}_4$. But even in this cases the occupied orbitals are typically of $3x^2 - r^2$ and $3y^2 - r^2$ type, not $x^2 - y^2$. [10] Thus this conclusion of Ref. 6 is extremely unusual, and it could be very important to understand the reasons of such a behavior. This could have a fundamental importance for the large class of materials and phenomena, connected with the behavior of systems with JT ions and with orbital ordering - phenomena which play more and more important role in modern solid state physics. [11]

In the present paper magnetic, electronic and structural properties of $\text{NaMn}_7\text{O}_{12}$ were studied using *ab initio* band structure calculations. We show that the charge ordering indeed occurs in the low temperature phase, but experimentally claimed [6] magnetic and crystal structures are inconsistent with each other. Performing the optimization of the atomic positions and unit cell vectors with fixed volume we found a new crystal structure consisting of the elongated MnO_6 octahedra. The orbital correlations resulting in such a structure are shown to exist even in a nondistorted cubic lattice. Thus, $\text{NaMn}_7\text{O}_{12}$ is not an exception from the general rule of only elongated octahedra for e_g degenerate Jahn-Teller ions, formulated above.

Crystal and magnetic structure.— It is worthwhile to rewrite the chemical formula of this compound as $(\text{NaMn}_3^{3+})(\text{Mn}_2^{3+}\text{Mn}_2^{4+})\text{O}_{12}$, which shows the relationship to the perovskite structure ABO_3 . Thus a part of the Mn^{3+} (d^4) ions occupies A positions (Mn_A^{3+}) in

initial perovskite structure having square surrounding, while the rest of the Mn ions are situated in the octahedral B sites (Mn_B^{3+} and Mn_B^{4+}). The checkerboard in the ac plane charge order of Mn_B develops below ~ 180 K (see Fig. 1 in Ref. 6). Mn chains of the same valence are formed along the b axis.

Above transition to the charge ordered state $\text{NaMn}_7\text{O}_{12}$ is paramagnetic (PM) and does not show long range magnetic order down to $T=125$ K, when the spins of the octahedral Mn form AFM-CE type structure [6, 12]. With further decrease of the temperature below 90 K also the Mn_A^{3+} ions order in the antiferromagnetic centered AFM state.

Details of the calculations.— Crystallographic data used in the calculations were taken from the Ref. 6. We used the Linear muffin-tin orbitals (LMTO) method [13] for the calculation in the experimental structure. The relaxation of this structure was performed using pseudopotential (PP) Vienna ab initio simulation package (VASP) [14] in the frameworks of the projector augmented wave method [15].

In spite of the fact that both methods (LMTO and PP) are not full-potential, they were successfully used previously for the study of the Jahn-Teller effects [16–19]. The potential in the LMTO is spherical, but kinetic part retains the symmetry of the lattice giving rise to appropriate orbital pattern as it will be shown below.

The von Barth-Hedin [20] and Perdew-Burke-Ernzerhof (PBE) [21] versions of the exchange-correlation potentials were utilized in the LMTO and PP calculations respectively. The strong Coulomb correlations were taken into account via the LSDA+U (for LMTO) and GGA+U (for PP) methods. [22] The values of on-site Coulomb interaction (U) and Hund's rule coupling (J_H) parameters were taken to $U=4.5$ eV $J_H=0.9$ eV. [23] The integration in the course of the self-consistency was performed over a mesh of 144 \mathbf{k} -points in the irreducible part of the Brillouin-zone. The ionic relaxation was performed using conjugate-gradient algorithm with convergence criteria for the total energy 10^{-4} eV.

We utilized Lichtenstein's exchange interaction parameter (LEIP) calculation procedure [24] for the Heisenberg Hamiltonian, which is written as $H = \sum_{ij} J_{ij} \vec{S}_i \vec{S}_j$. Summation here runs twice over every pair i, j .

Low temperature phase, experimental structure.— We start the investigation of $\text{NaMn}_7\text{O}_{12}$ with the LSDA+U calculations of the low temperature (LT) experimental structure. The total and partial densities of states (DOS) obtained for the AFM-CE type of magnetic order are shown in Fig. 1. It is easy to see that indeed two octahedral Mn ions show different charge states, which agrees with experimental expectations. [6]

One class of the octahedral Mn_B ions has $t_{2g}^3 e_g^1$ (i.e. Mn_B^{3+}) configuration with the half-filled $x^2 - y^2$ orbital

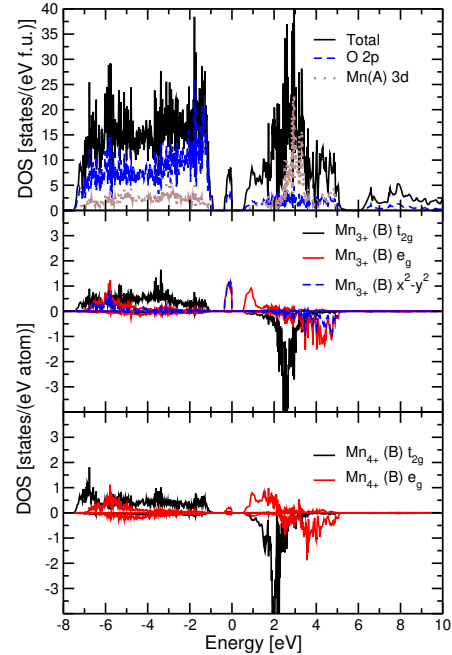


FIG. 1: (color online). Results of the LSDA+U calculation (LMTO) for the low temperature experimental crystal structure (compressed Mn^{3+}O_6 octahedra): total and partial densities of states (DOS). AFM-CE type of the magnetic structure was used. Fermi energy is in zero.

(middle panel in Fig. 1). The top of the valence band is defined exactly by these states. This in turn agrees with the crystal field theory: the compression of the MnO_6 octahedra along local z -axis should result in the crystal field splitting of the e_g shell, such that the $3z^2 - r^2$ goes higher in energy and an electron localizes on the $x^2 - y^2$ orbital. The detailed analysis of the occupation matrices shows that the occupied orbital is the same for all octahedral Mn_B^{3+} ions. The local magnetic moment on this Mn equals $3.4 \mu_B$. It is reduced with respect to ionic value ($4 \mu_B$) due to hybridization with O 2p states, which is clearly seen in the DOS plot in the range from -7 to -5 eV (most pronounced for the e_g states.)

Another class of the octahedral Mn ions shows valence state 4+ with basically empty e_g shell (there is however some occupation of these states due to hybridization with oxygen), see lowest panel in Fig. 1. The magnetic moment on this ion equals $2.9 \mu_B$.

The orbital ordering obtained in the distorted LT phase is presented in Fig. 2. One may see, that indeed the single electron in the e_g shell of Mn_B^{3+} ions is stabilized on the $x^2 - y^2$ orbital. Since the orbital is the same on each Mn_B^{3+} , one may expect that the exchange interaction in the ac plane will be FM (exchange between half-filled and

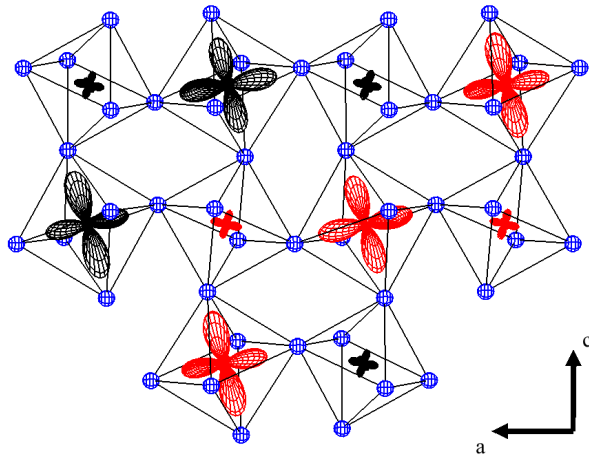


FIG. 2: (color online). Orbital order in the octahedral Mn_B sublattice realized in the LSDA+U (LMTO) calculations of the low temperature phase with experimental distortions (compressed MnO_6 octahedra). The occupied e_g orbitals are shown. Magnetic order was chosen to be of AFM-CE type. Black and red orbitals correspond to different spins. Blue balls are oxygens. The Mn_B^{4+} ions are sitting in the corners of the zig-zag chains, while Mn_B^{3+} in the middle of the zig-zag bars.

empty e_g orbitals of Mn_B^{3+} and Mn_B^{4+} respectively) [25] with *all* neighboring Mn_B , not only with those forming zig-zag chain. Thus, this orbital order should stabilize FM, not AFM-CE type of magnetic ordering in the ac plane.

In order to check this proposal we calculated the exchange constants with the use of the LEIP formalism. This method allows not only to find all exchange parameters in one magnetic calculation, but also to analyze, how stable is a given magnetic configuration (see e.g. Ref. 26). The exchange constants between the octahedral Mn_B^{3+} - Mn_B^{4+} ions within one zig-zag chain was found to be $J_1 \sim -7 \div 10$ K, all FM. For the AFM-CE type of the magnetic order the coupling between chains, J_2 , is expected to be AFM, but LEIP calculation shows that J_2 could be AFM or FM, depending on particular pair: $|J_2| \sim 3 \div 6$ K. Thus this magnetic structure is unstable within LEIP. [26] The total energy calculations indeed show that e.g. AFM- A_{ac} (ferromagnetic ac planes) solution is lower in energy than AFM-CE (on 22 meV/f.u.).

To sum up in contrast to naive expectations the experimental LT crystal structure leads to the orbital ordering inconsistent with the experimental magnetic order, the real band structure calculations also show that AFM-CE type of the magnetic structure does not corresponds to the lowest total energy.

Orbital order in cubic structure.— In order to resolve this inconsistency we performed the calculation for the cubic structure, taken from the HT phase, but with the cell volume corresponding to the LT one. The magnetic

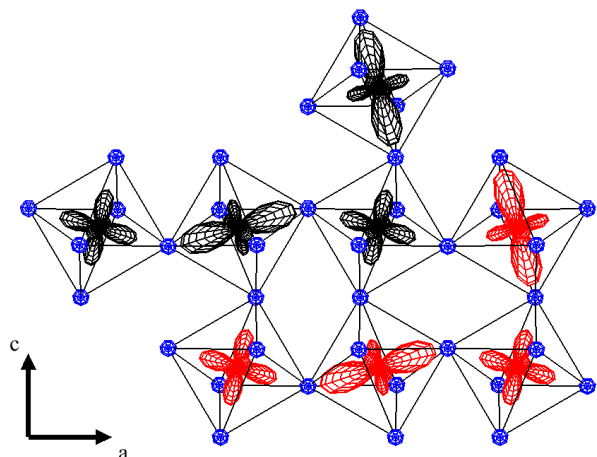


FIG. 3: (color online). Orbital order in the octahedral Mn_B sublattice realized in the LSDA+U (LMTO) calculations of the high temperature, cubic phase (prior to the lattice optimization). Magnetic order was chosen to be AFM-CE type. The occupied e_g orbitals are shown. Color coding is the same as in Fig. 2.

structure is experimental, AFM-CE in the ac plane for the Mn_B and antiferromagnetic for Mn_A . The orbital ordering in the e_g shell obtained is shown in Fig. 3. One may see two distinct features different from the results for the experimental LT crystal structure (i.e. with Fig. 2).

First of all, there is no clear charge order in this structure, which is seen from the substantial charge density on the corners of the zig-zags, the Mn_B^{4+} ions in the LT experimental structure. This is related with equal volumes of all oxygen octahedra surrounding Mn ions sitting in the B sites in this cubic structure.

The second difference is more important. Even in the absence of the corresponding distortions of the MnO_6 octahedra the single half-filled orbital in the e_g shell of the Mn_B^{3+} ions is of the $3z^2 - r^2$ symmetry (actually these are alternating $3x^2 - r^2$ and $3y^2 - r^2$ orbitals). Thus the exchange coupling alone (without lattice distortions) stabilizes a certain orbital order. This orbital pattern is fully consistent with the Goodenough-Kanamori-Anderson rules. [25] It explains the ferromagnetic (FM) coupling in the zig-zag chains and antiferromagnetic (AFM) between them (due to the half-filled t_{2g} orbitals).

However, stabilization of the $3z^2 - r^2$ orbital should lead to a certain distortion of the $\text{Mn}_B^{3+}\text{O}_6$ octahedra: elongation in the ac plane. In order to check this hypothesis we performed the optimization of the atomic positions and cell shape keeping the volume constant and equal to the volume of the unit cell in the LT phase. The calculations were performed using VASP code within the GGA+U approximation.

Lattice optimization.— The $\text{Mn}_B^{3+}\text{O}_6$ octahedra in the

TABLE I: Total energies and absolute values of spin moments on the Mn ions for different magnetic configurations in the ac plane. The atomic positions and the unit cell shape were relaxed for each magnetic structure in the GGA+U calculation. Experimental magnetic order for the Mn_A ions and AFM order of spins for Mn_B in the b direction were used. We checked that for FM coupling along the b axis AFM-CE type of also provides the lowest total energy.

	Total energy (meV/f.u.)	Magnetic moments (μ_B)		
		Mn_A^{3+}	Mn_B^{3+}	Mn_B^{4+}
AFM-CE	0	3.8	3.6	3.0
AFM- A_{ac}	58	3.8	3.7	3.1
AFM- C_{ac}	72	3.8	3.6	2.9
AFM- G_{ac}	123	3.8	3.7	2.8

optimized structure for the AFM-CE type indeed turn out to be elongated, not compressed (corresponding crystal structure data are given in the Supplemental Materials [27]). There are two long (2.08 Å) and four short (two 1.93 Å and two 1.92 Å) Mn_B^{3+} -O bonds. The $\text{Mn}_B^{4+}\text{O}_6$ octahedra stays to be slightly distorted (Mn-O bond lengths are 1.92×2 , 1.93, 1.91, 1.88, and 1.87 Å). The total energy of the optimized structure for the AFM-CE type of magnetic order is on 81 meV/f.u. lower than experimental one.

The magnetic moments on two types of the Mn ions sitting in the B sites (in the middle of the bar and in the corner of the zig-zags) were found to be 3.6 and 3.0 μ_B , which certifies the presence of the charge ordered state. The band gap equals ~ 0.7 eV.

As it was discussed above for AFM-CE the stabilization of the $3x^2 - r^2$ and $3y^2 - r^2$ orbitals ordering is favorable. It coexists with the lattice distortion with locally elongated $\text{Mn}_B^{3+}\text{O}_6$ octahedra. The mechanism of such ordering could be superexchange interaction, [28] but it could be also elastic interaction of locally distorted Jahn-Teller centers. [29]

Since the strength of the superexchange interaction depends on the on-site Hubbard repulsion we repeated lattice relaxation for much larger value of $U = 8$ eV and found that even for this U octahedra surrounding Mn_B^{3+} ions are elongated in the optimized structure.

However, there may exist other types of the magnetic ordering in the ac plane for Mn_B , which may result in different orbital pattern and different lattice distortions (this occurs e.g. for AFM- A_{ac}). To check this possibility we carried out the crystal structure optimization for the AFM- A_{ac} , AFM- C_{ac} (FM chains in the ac plane), and AFM- G_{ac} (all neighbors in the ac plane are AFM). One may see from Tab. I that these three types of the magnetic structure are higher in energy than the experimental AFM-CE type.

The situation in $\text{NaMn}_7\text{O}_{12}$ reminds that in K_2CuF_4 , in which on the basis of net tetragonal compression with $c/a < 1$ it was initially concluded that the CuF_6 octa-

hedra are compressed in the c direction, so that K_2CuF_4 was even cited in the textbooks as the only example with Cu^{2+} in compressed octahedra. [25, 30] But it was later shown theoretically [31] and confirmed experimentally [32] that actually CuF_6 octahedra are elongated, but with long axes oriented in the a and b directions.

Discussion.— Our results demonstrate that the situation in the ordered phase of $\text{NaMn}_7\text{O}_{12}$ should be different from that deduced in Ref. 6: whereas the observed charge and magnetic ordering of the CE type are reproduced in our calculation, the orbital order obtained theoretically is completely different from the one previously proposed. Instead of the $x^2 - y^2$ orbitals, occupied at all Mn_B^{3+} ions, we obtained that the $3x^2 - r^2$ and $3y^2 - r^2$ orbitals should be occupied, forming stripe pattern of the same type as in the more conventional half-doped manganites like $\text{La}_{0.5}\text{Ca}_{0.5}\text{MnO}_3$.

Such an orbital order naturally explains the AFM-CE type of the magnetic structure, observed experimentally, whereas the $x^2 - y^2$ orbital ordering proposed in Ref. 6 would give ferromagnetic ac planes. The orbital order obtained in the present paper is accompanied (or is caused by) corresponding changes of the crystal lattice with not compressed, but elongated MnO_6 octahedra, with long axes alternating in x and y (i.e. a and c) directions. The *average* distortion in this case is also a contraction of the unit cell in the b direction, as it was found experimentally, [6] but with this average contraction being not due to respective compression of the MnO_6 octahedra along b , but rather elongation in the a and c directions. More careful structural studies, as well as e.g. NMR or XAS measurements are expected to reveal corresponding extra lattice distortions predicted by the present calculations.

In effect it turns out that the general rule that the local distortions around Jahn-Teller centers with double degeneracy always correspond to local elongation, is also valid in this system, so that it seems to be valid without any known exceptions. This general message should be kept in mind in studying other systems with double e_g orbital degeneracy.

Acknowledgments.— S.S. is grateful to M. Korotin, who showed us long ago his results on the study of the charge and spin states of the Mn ions in this materials and to A. Gubkin and E. Sherstobitova for useful discussions about the symmetry of the crystal lattice of $\text{NaMn}_7\text{O}_{12}$. This work is supported by the Russian Foundation for Basic Research via RFFI-13-02-00374, RFFI-13-02-00050, the Ministry of education and science of Russia (MK-3443.2013.2). The part of the calculations were performed on the “Uran” cluster of the IMM UB RAS.

* Electronic address: streltsov@imp.uran.ru

[1] C. C. Homes, T. Vogt, S. M. Shapiro, S. Waki-

- moto, and A. P. Ramirez, Science (New York, N.Y.) **293**, 673 (2001), ISSN 0036-8075, URL <http://www.ncbi.nlm.nih.gov/pubmed/11474105>.
- [2] Y. W. Long, N. Hayashi, T. Saito, M. Azuma, S. Muranaka, and Y. Shimakawa, Nature **458**, 60 (2009), ISSN 1476-4687, URL <http://www.ncbi.nlm.nih.gov/pubmed/19262669>.
- [3] R. D. Johnson, L. C. Chapon, D. D. Khalyavin, P. Manuel, P. G. Radaelli, and C. Martin, Physical Review Letters **108**, 067201 (2012), ISSN 0031-9007, URL <http://link.aps.org/doi/10.1103/PhysRevLett.108.067201>.
- [4] N. Perks, R. Johnson, C. Martin, L. Chapon, and P. Radaelli, Nature Communications **3**, 1277 (2012), ISSN 2041-1723, URL <http://www.nature.com/doifinder/10.1038/ncomms2294>.
- [5] F. Mezzadri, M. Buzzi, C. Pernechele, G. Calestani, M. Solzi, A. Migliori, and E. Gilioli, Chemistry of Materials **23**, 3628 (2011), URL <http://pubs.acs.org/doi/abs/10.1021/cm200879p>.
- [6] A. Prodi, E. Gilioli, A. Gauzzi, F. Licci, M. Marezio, F. Bolzoni, Q. Huang, A. Santoro, and J. W. Lynn, Nature Materials **3**, 48 (2004).
- [7] J. Kanamori, Journal of Applied Physics **31**, 14S (1960), URL http://ieeexplore.ieee.org/xpls/abs_all.jsp?arnumber=5123663.
- [8] D. Khomskii and J. van den Brink, Phys. Rev. Lett. **85**, 3329 (2000), URL <http://link.aps.org/doi/10.1103/PhysRevLett.85.3329>.
- [9] I. B. Bersuker, *The Jahn-Teller effect* (Cambridge University Press, Cambridge, 2006).
- [10] H. Wu, C. Chang, O. Schumann, Z. Hu, J. Cezar, T. Burnus, N. Hollmann, N. Brookes, A. Tanaka, M. Braden, et al., Physical Review B **84**, 155126 (2011), ISSN 1098-0121, URL <http://link.aps.org/doi/10.1103/PhysRevB.84.155126>.
- [11] N. Nagaosa and Y. Tokura, Science **288**, 462 (2000), ISSN 00368075, URL <http://www.sciencemag.org/cgi/doi/10.1126/science.288.5462.462>.
- [12] A. Gauzzi, E. Gilioli, A. Prodi, F. Bolzoni, F. Licci, M. Marezio, G. L. Calestani, M. Affronte, Q. Huang, A. Santoro, et al., Journal of Superconductivity **18**, 675 (2005).
- [13] O. K. Andersen and O. Jepsen, Phys. Rev. Lett. **53**, 2571 (1984), URL <http://link.aps.org/doi/10.1103/PhysRevLett.53.2571>.
- [14] G. Kresse and J. Furthmüller, Physical Review B **54**, 11169 (1996), ISSN 0163-1829, URL <http://www.ncbi.nlm.nih.gov/pubmed/9984901>.
- [15] P. E. Blöchl, Physical Review B **50**, 17953 (1994), URL http://prb.aps.org/abstract/PRB/v50/i24/p17953_1.
- [16] N. Binggeli and M. Altarelli, Phys. Rev. B **70**, 085117 (2004).
- [17] G. Trimarchi and N. Binggeli, Phys. Rev. B **71**, 035101 (2005).
- [18] J. E. Medvedeva, M. A. Korotin, V. I. Anisimov, and A. Freeman, Physical Review B **65**, 172413 (2002), ISSN 0163-1829, URL <http://prb.aps.org/abstract/PRB/v65/i17/e172413>.
- [19] S. V. Streltsov and D. I. Khomskii, Phys. Rev. B **86**, 035109 (2012).
- [20] U. von Barth and L. Hedin, Journal of Physics C: Solid State Physics **5**, 1629 (1972), URL <http://iopscience.iop.org/0022-3719/5/13/012>.
- [21] J. P. Perdew, K. Burke, and M. Ernzerhof, Phys. Rev. Lett. **77**, 3865 (1996), ISSN 1079-7114, URL <http://www.ncbi.nlm.nih.gov/pubmed/10062328>.
- [22] V. I. Anisimov, F. Aryasetiawan, and A. I. Liechtenstein, J. Phys.: Condens. Matter **9**, 767 (1997), URL <http://iopscience.iop.org/0953-8984/9/4/002>.
- [23] S. V. Streltsov and D. I. Khomskii, Physical Review B **77**, 064405 (2008), ISSN 1098-0121, URL <http://link.aps.org/doi/10.1103/PhysRevB.77.064405>.
- [24] A. I. Liechtenstein, V. Gubanov, M. Katsnelson, and V. Anisimov, Journal of Magnetism and Magnetic Materials **36**, 125 (1983).
- [25] J. B. Goodenough, *Magnetism and the Chemical Bond* (Interscience publishers, New York-London, 1963).
- [26] Z. V. Pchelkina and S. V. Streltsov, Physical Review B **88**, 054424 (2013), ISSN 1098-0121, URL <http://link.aps.org/doi/10.1103/PhysRevB.88.054424>.
- [27] S. Streltsov and D. Khomskii, Supplemental Materials (2014).
- [28] K. I. Kugel and D. I. Khomskii, Soviet Physics Uspekhi **25**, 231 (1982), ISSN 0042-1294.
- [29] A. O. Sboychakov, K. I. Kugel, A. L. Rakhmanov, D. I. Khomskii, Physical Review B **83**, 205123 (2011), ISSN 1098-0121, URL <http://link.aps.org/doi/10.1103/PhysRevB.83.205123>.
- [30] C. J. Ballhausen, *Introduction to Ligand Field Theory* (McGraw-Hill, New York, 1962).
- [31] D. Khomskii and K. Kugel, Solid State Communications **13**, 763 (1973), URL <http://www.sciencedirect.com/science/article/pii/0038109873>.
- [32] Y. Ito and J. Akimitsu, J. Phys. Soc. Jpn. **40**, 1333 (1976).